Low Radio Frequency Spatially Resolved Studies of Nearby Galaxies : Magnetic Field

Souvik Manna

Supervisor : Subhashis Roy

Outline

- Introduction
- Measurement of magnetic field
- Low radio frequency observation
- Sample selection
- Results
- Propagation of cosmic ray particles
  - Thin disk approximation
  - Thick disk approximation
- Conclusion and future work

Introduction:

- Magnetic field has effect at every scale in the star formation process:
  - Dynamics of the galactic ISM.
  - Collapse of turbulent molecular clouds.
  - Fragmentation of individual starforming cores.

(Elmegreen 1981 ; Crutcher 1999 ; Price et al. 2008)

- Density, distribution and motion of cosmic ray particles.
- Confinement of charged particles within galaxies. **(Adebahr et al. 2012)**
- **Origin :**
- Seed field was amplified by compression during collapse and shearing by a differentially rotating disk. **(Beck 2006)**
- Dynamo action within the galaxy amplifies and maintains field strength over galactic lifetime.

(Moffatt 1978; Parker 1979; Subramanian, 2008; Shukurov et al. 2006)

- Magnetohydrodynamic (MHD) turbulence can amplify the local magnetic field. **(Batchelor 1950; Groves et al. 2003)**

Measurement of magnetic field

- B in the sky plane can be estimated from intensity of Synchrotron radiation through minimum energy condition.

  (Burbidge 1956)

- Magnetic energy $\sim B^2 / 8\pi$.
- Particle energy can be calculated from N(E)dE.
- Magnetic field can only be estimated at the minimum energy condition.
- Particle and magnetic energy are in **equipartition** at minimum energy condition.
- We have used revised equipartition formula by Beck & Krause 2005.
- **Flux density** and **spectral index** map is required.

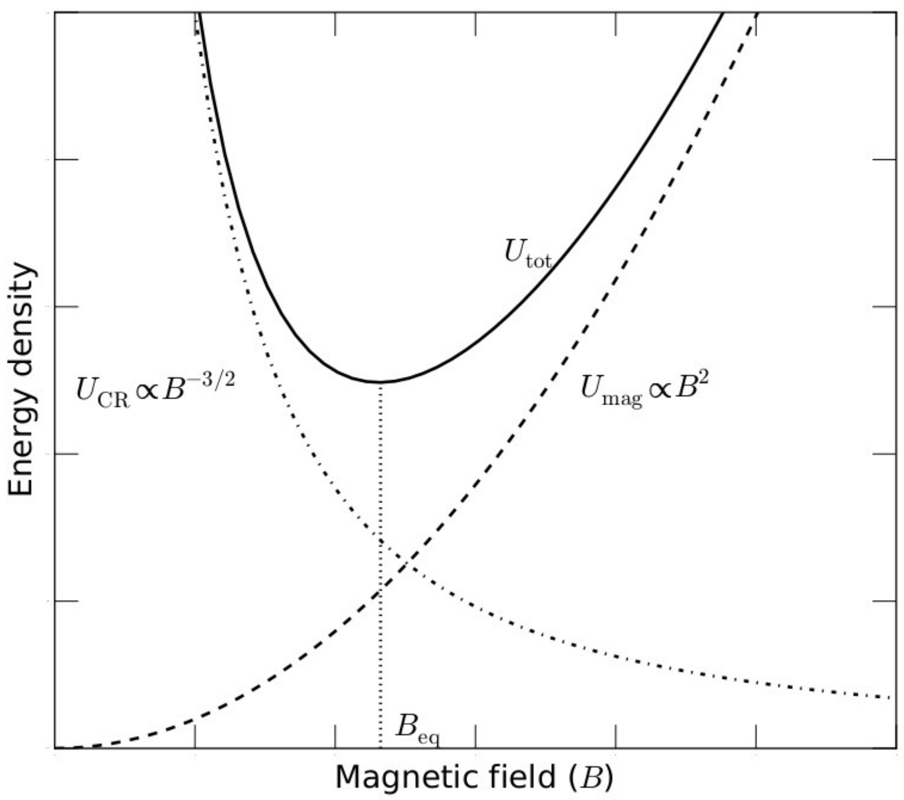

Credit : Aritra Basu

$$B_{eq} = \left\{ 4\pi (K_0 + 1) E_p^{1-2\alpha_{nt}} \frac{f(\alpha_{nt})}{c_4(i)} \frac{I_\nu \nu^{\alpha_{nt}}}{l} \right\}^{1/(\alpha_{nt}+3)}$$

Low radio frequency observation

- In NGC253, magnetic field was found to be ~20uG in the centre and dropped to 8uG towards the edge. **(Heesen et al. 2009)**
- In M82, the total field was found to be ~80 μG in the centre and ~20–30 μG in the synchrotron emitting halo. **(Adebahr et al. 2012)**
- **Basu et al. 2013** studied 5 nearby face-on spirals and found their **equipartition magnetic field** to be of ~25 uG in the central region, which falls by a factor of 2 at the outer disks. The energy density in the magnetic field was found to be similar to gaseous energy density.
- However, spatially resolved magnetic fields for most of the nearby galaxies (especially for different **Hubble** types) have not been studied.
- **Thermal free-free emission contribution is much lower below L band frequency due to steep spectral indices of non-thermal emission.**
- **Once the thermal radio emission from galaxies have been modelled and subtracted from total radio emission, the resultant non-thermal emission provides :**
    - Non-thermal spectral index from multiband radio observations.
    - Sky plane magnetic field through minimum energy condition.
    - Radial scale length , verticle scale height etc. to study the mechanism of propagation of low energy cosmic ray particles.

Sample selection

- Spitzer Local Volume Legacy (**LVL**) sample of 258 galaxies within 11 Mpc :
    - IR MIPS observations up to 160 μm.
    - UV, H-α and optical band data.

(Dale et al. 2009)

- 46 out of 258 galaxies of LVL sample were selected based on:
    - Galaxies of angular sizes between 6 arcmin (**large no of beams across galaxies**) and 17 arcmin (**to avoid zero-spacing problem**) well suited for the GMRT observations.
    - Declination > -45 degree to observe for more than 4 hours a day.
- We have analysed GMRT data at 330 MHz and VLA data at L- band for 7 galaxies.
- uGMRT observation of another 17 galaxies between 300-500 MHz of different hubble types in last cycle of GMRT.

Non-thermal radio emission

- Hα and 24μm maps were used to model thermal free-free radio emission and this thermal maps were subtracted from radio images to get **non-thermal radio emission.** **(Tabatabaei et al. 2007)**

- **Non-thermal spectral index** maps were generated using 1.4 GHz VLA image and 330 MHz GMRT image.

Non-thermal radio maps and spectral index

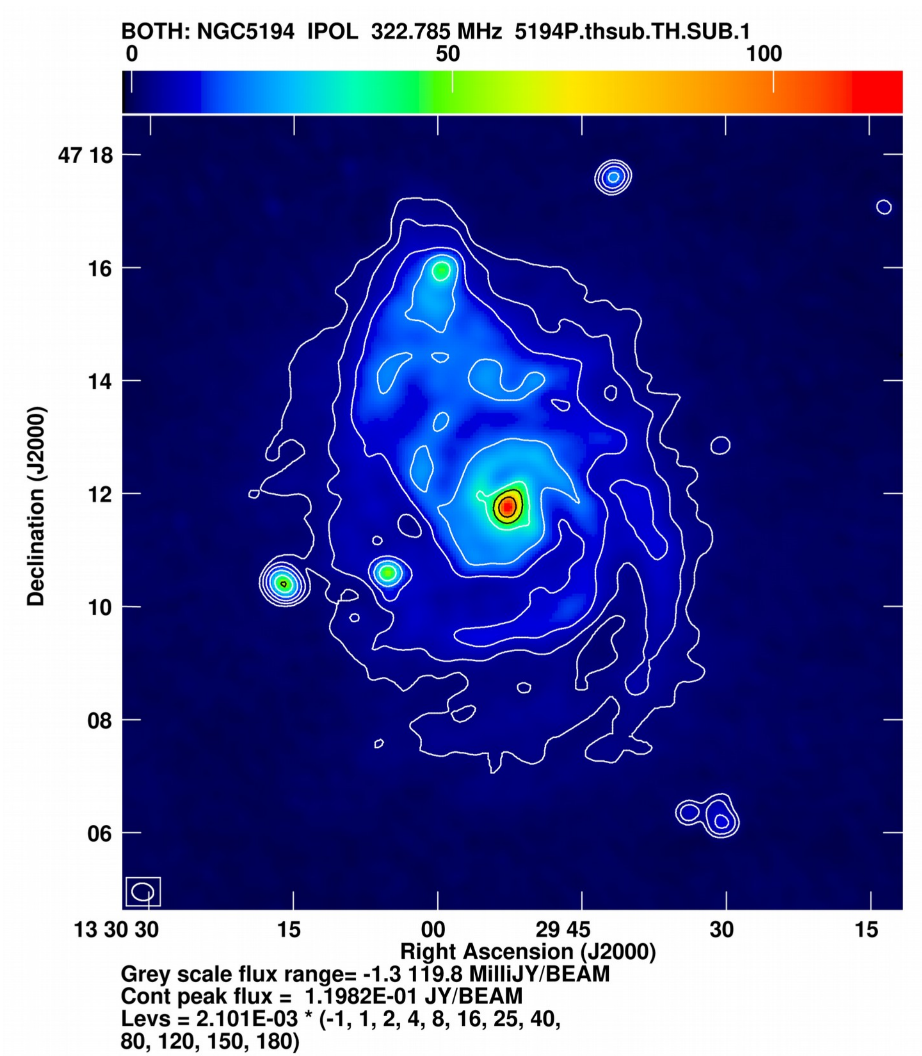

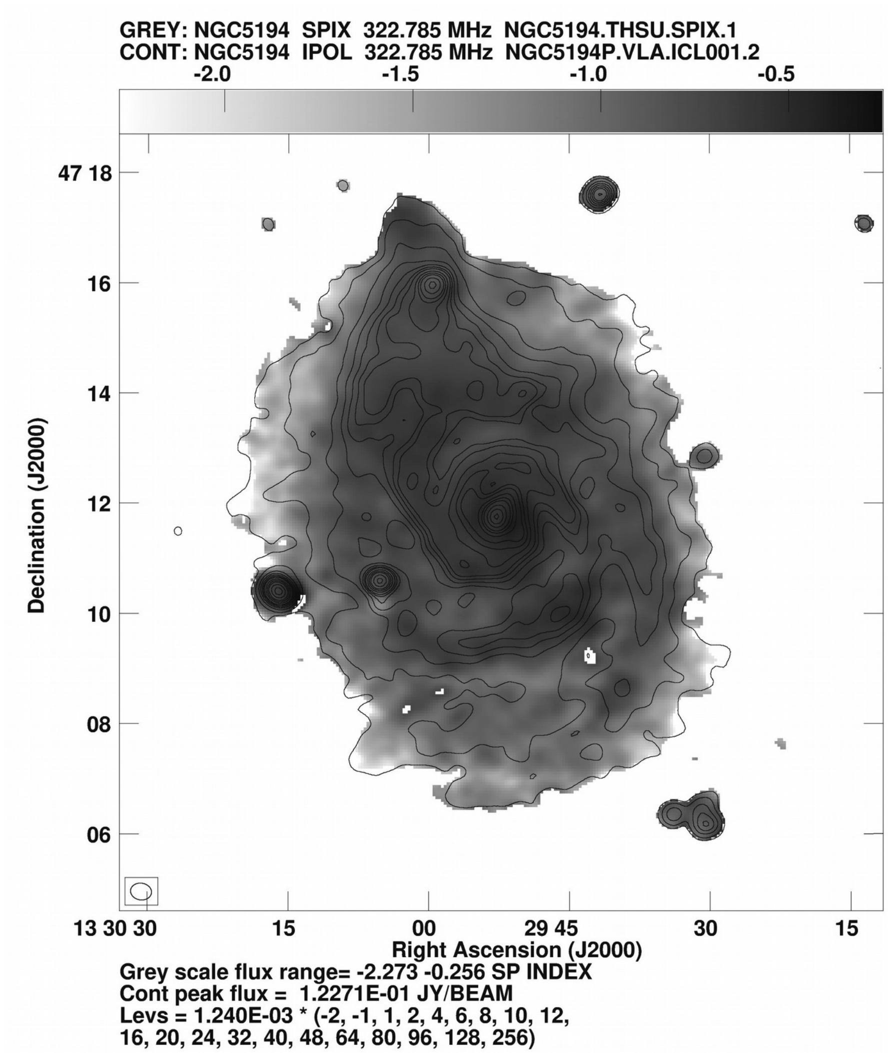

Results: Magnetic field maps and radial profile

$$B_{eq} = \left\{ 4\pi(K_0+1)E_p^{1-2\alpha_{nt}} \frac{f(\alpha_{nt})}{c_4(i)} \frac{I_\nu \nu^{\alpha_{nt}}}{l} \right\}^{1/(\alpha_{nt}+3)}$$

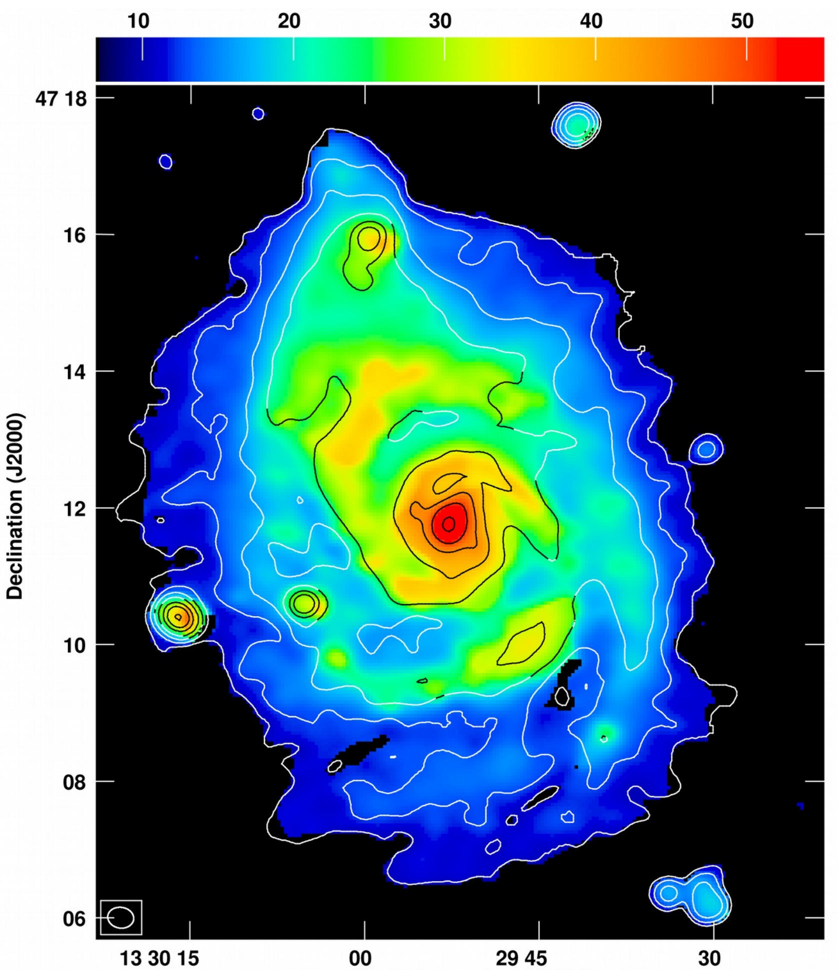

- We have projected an **ellipse** over the galaxy taking into account the position angle and inclination of the galaxy.
- Width of each annular region is equal to the beam size.
- We show B_{eq} averaged over each of the annuli.

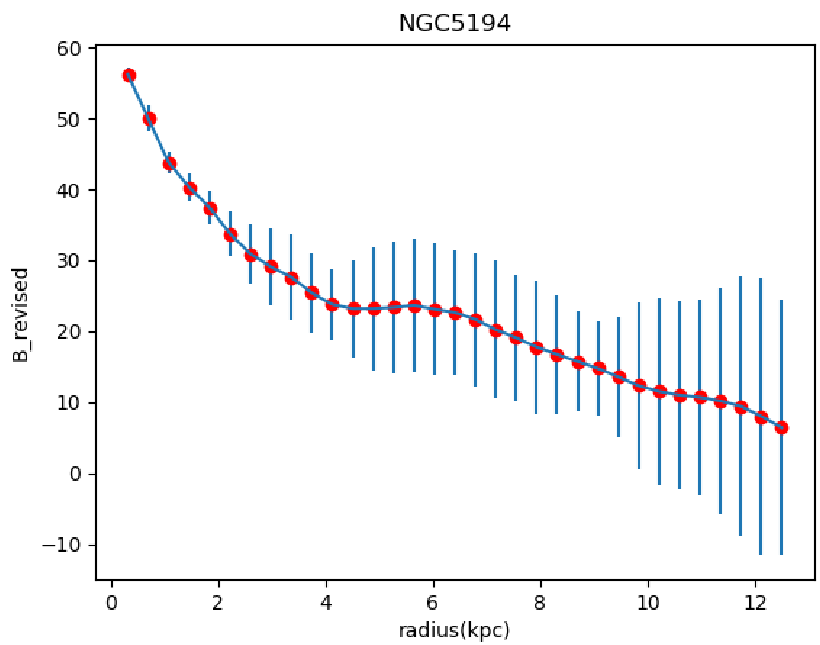

Results: Magnetic field maps and radial profile

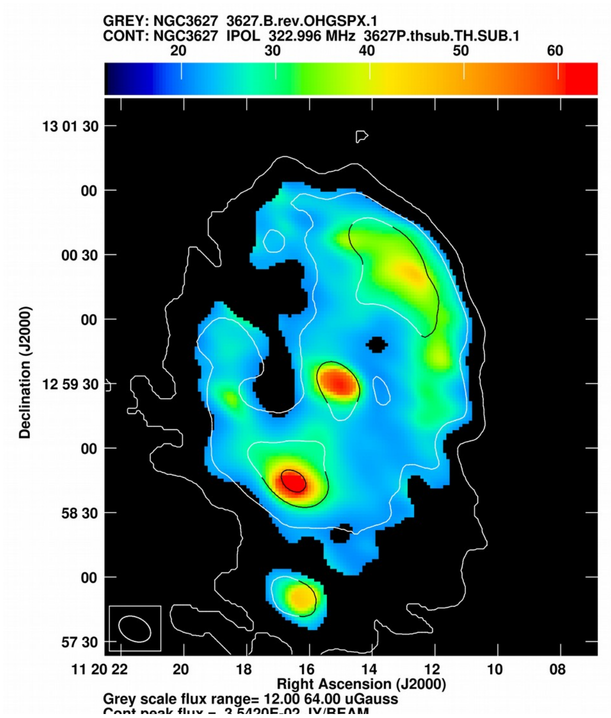

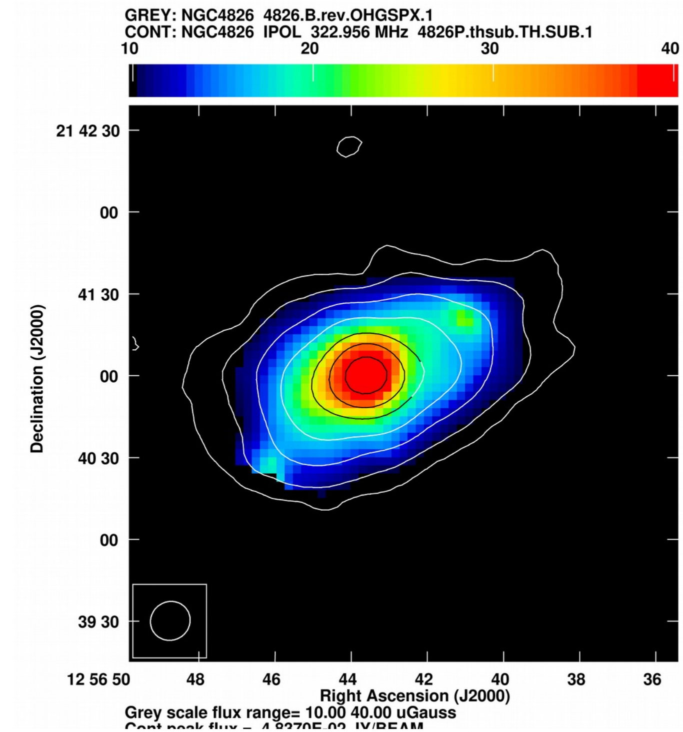

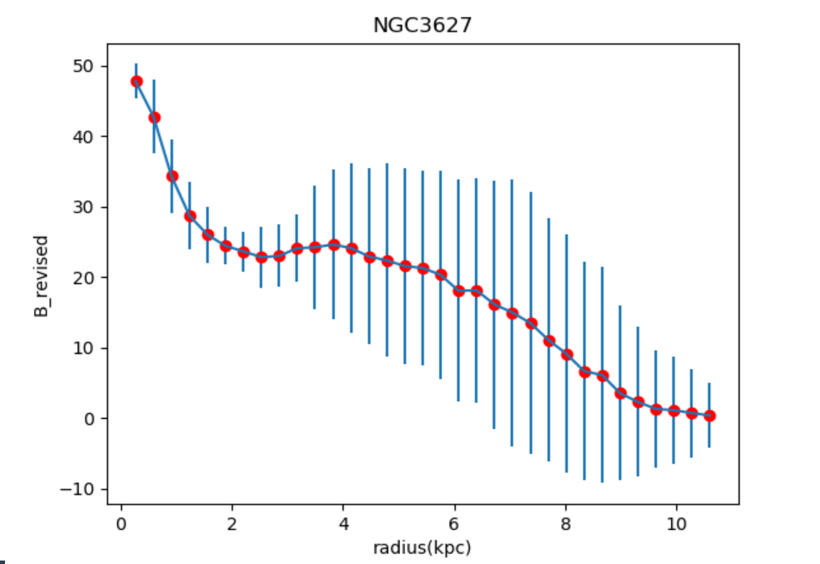

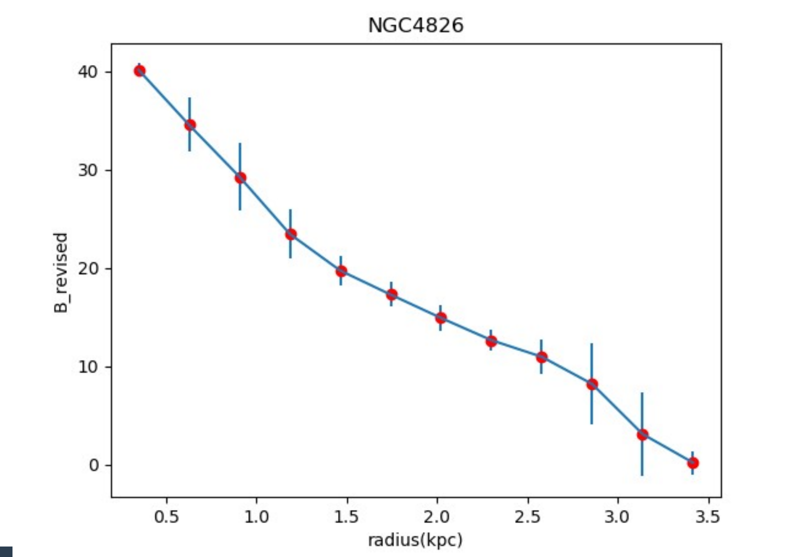

Results: Magnetic field maps and radial profile

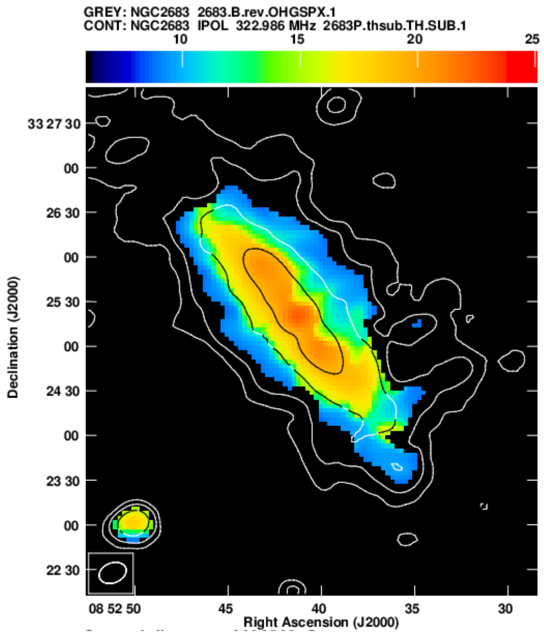

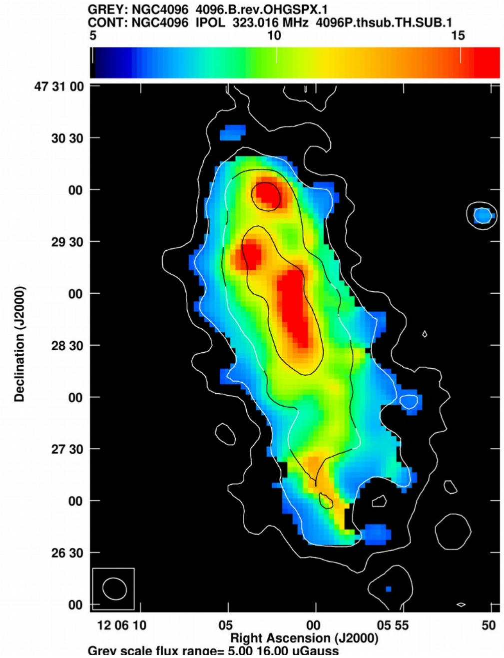

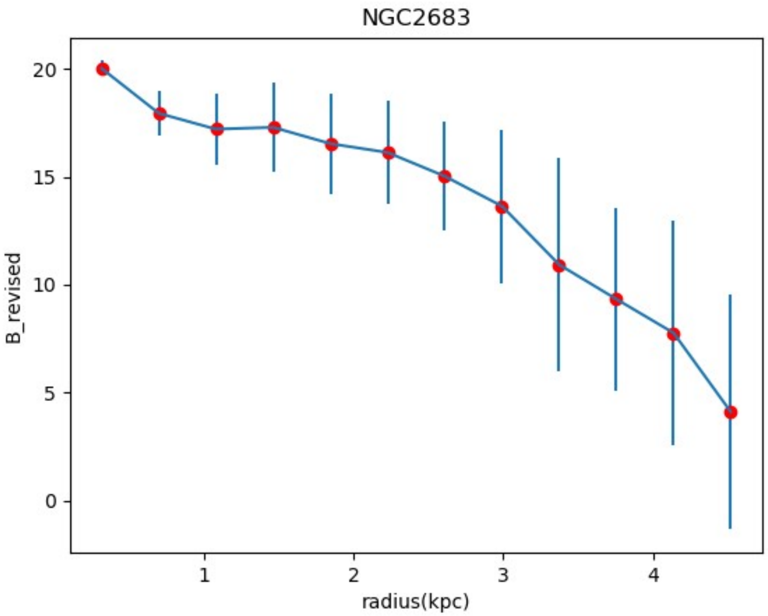

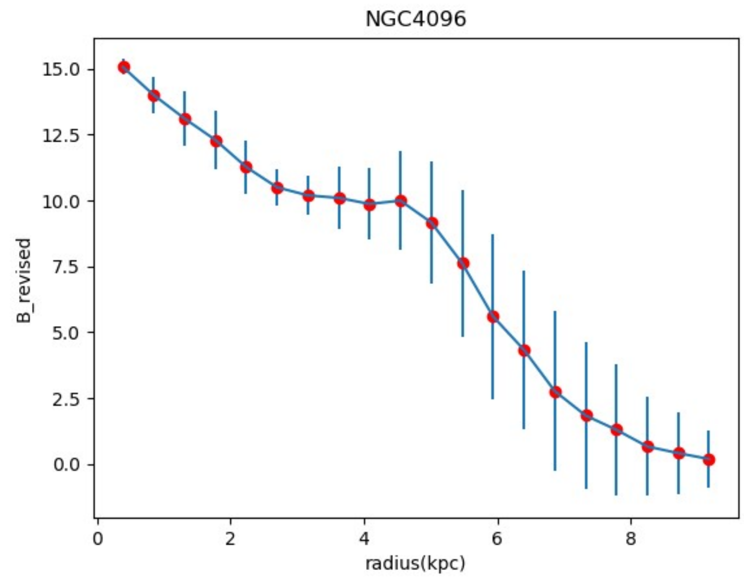

Results: Magnetic field maps and radial profile

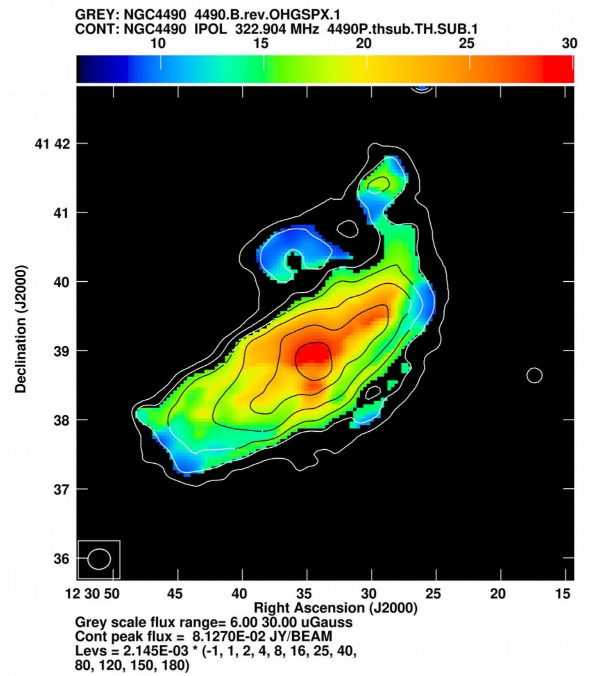

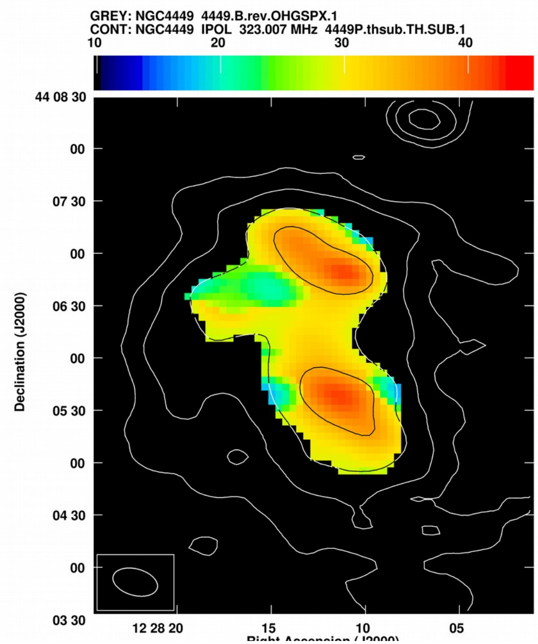

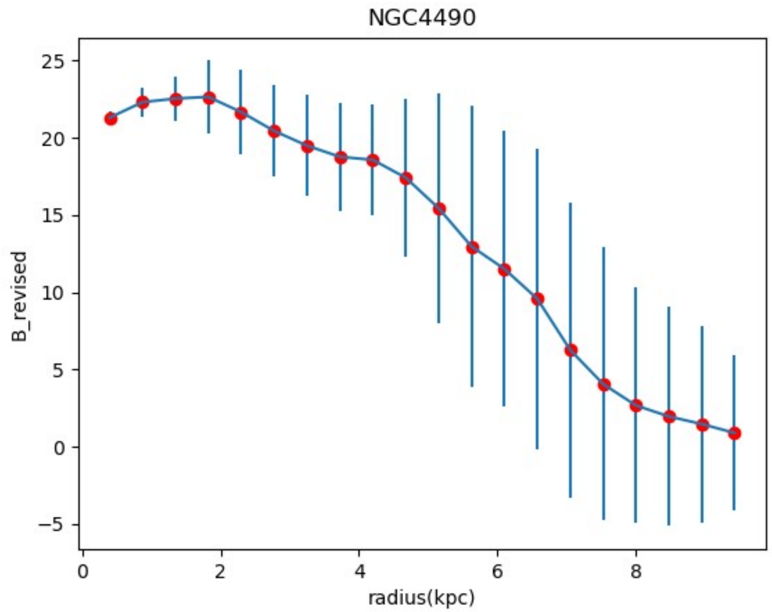

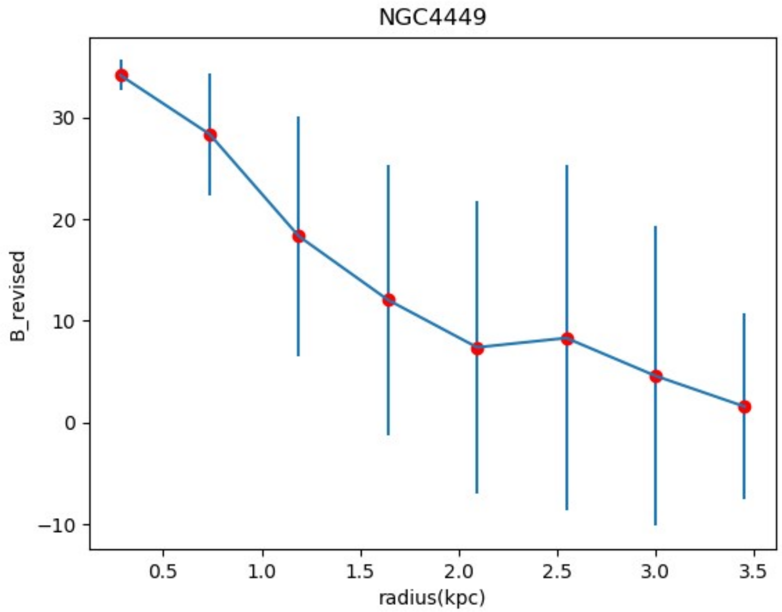

Magnetic field error estimation

- **Monte Carlo method:**
  - 10^4 random samples whose **mean is the flux density** of that pixel and **map noise was taken as rms**.
  - 10^4 realisations of spectral index is generated at each pixel using 90cm and 20cm radio maps.
  - Mean and rms of these spectral index values are respectively the mean spectral index and spectral index error of a single pixel.
  - Magnetic field maps and its error maps are generated using flux density and spectral index maps.
  - Revised equipartition formula diverges for spectral index of <0.5. We replace Spectral index values less than 0.55 by ‘nan’.

Error maps

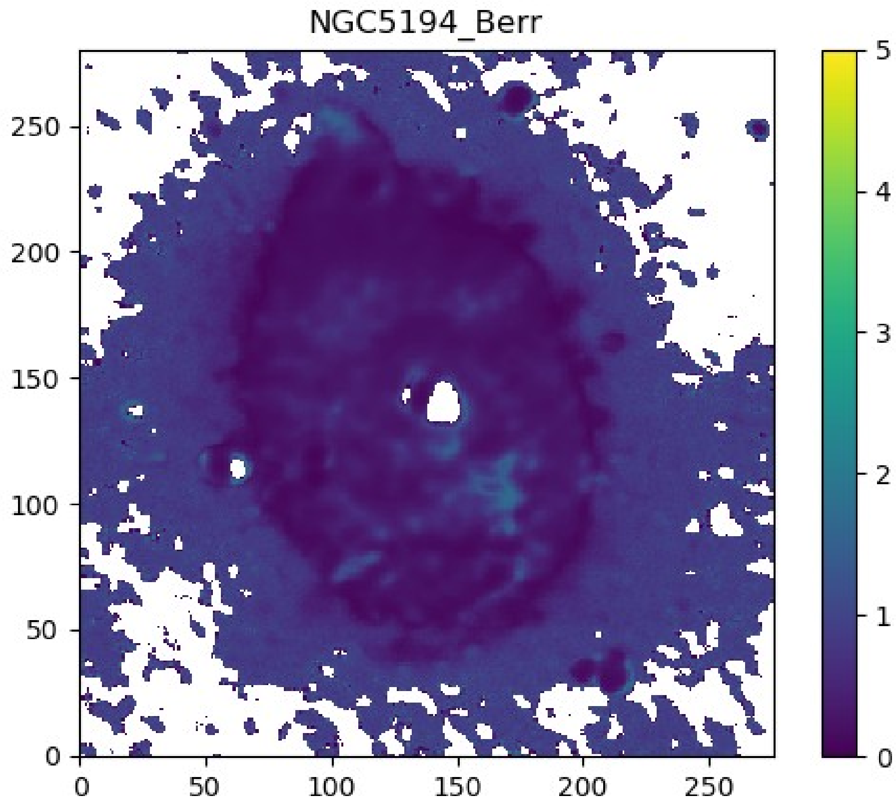

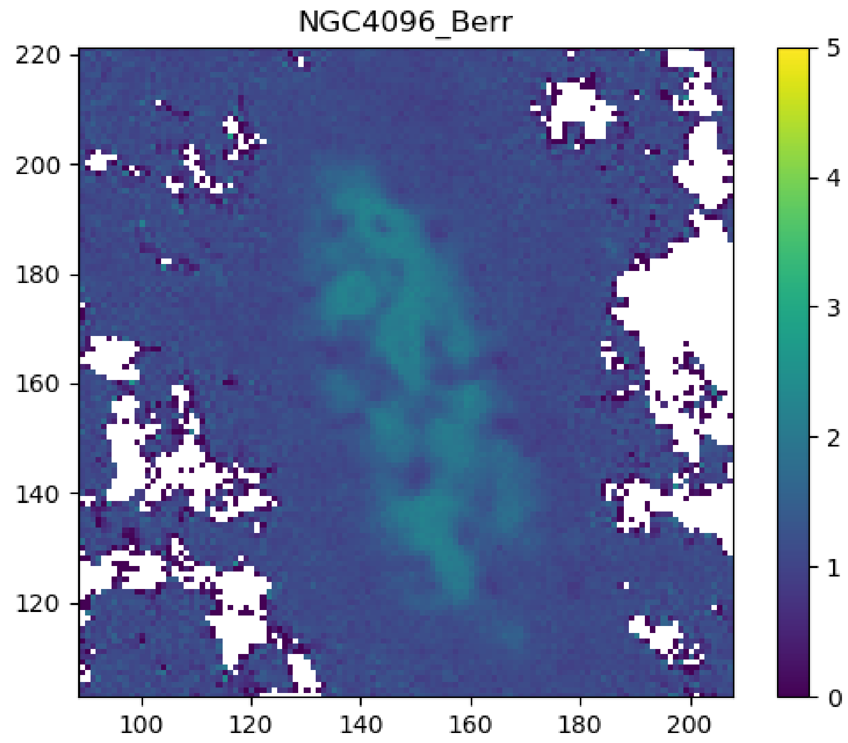

- Mean magnetic field errors are 7.3%, 6.1%, 15.0%, 18.5%, 10.6%, 18.1% and 8.0% for NGC5194. NGC3627, NGC4096, NGC4826, NGC4449, NGC2683, NGC4490 respectively.

Propagation of cosmic ray particles

- **Face on galaxies:**
  - Components : Central bulge and outer disk.
  - Radial scale length at the outer disk at different frequencies is required.
  - Fit suitable function on the radial profile assuming thin disk model.
- **Edge on galaxies:**
  - Disk distribution as well as vertical distribution : Radial scale length and vertical scale height.
  - Inclination of galaxy is also not known accurately.
- Exponential function is used earlier to estimate radial scale length.

  (Basu et al. 2013, Argyle et al. 2018)
- CHANG-ES : Scale height measurement of 13 edge on galaxies observed by EVLA in C and L band. **(Krause et al. 2017)**

Thin disk approximation : Radial scale length NGC5194 (face-on)

- Mean flux density is estimated over annular elliptical region having width of the beam size.
- Two main observed components of galaxies: Central bulge and outer disk.
- **$F = f_0 \exp(-r/r_0) + f_1 \exp(-r/r_1)$**

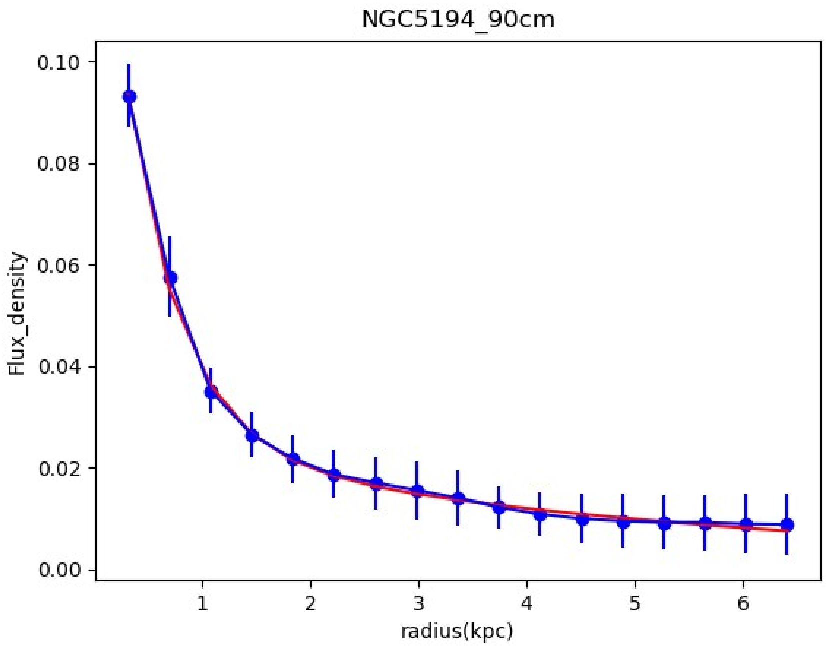

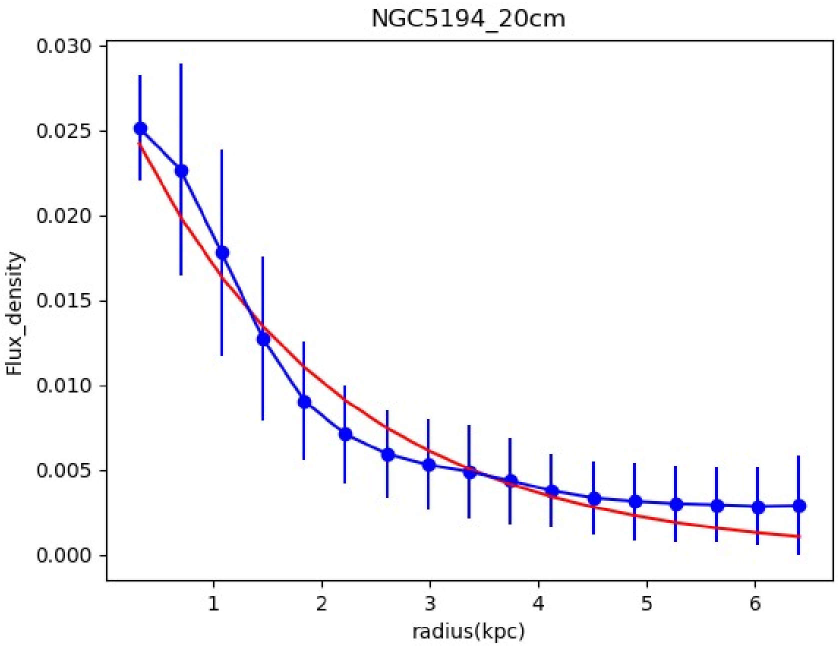

Thin disk approximation : Radial scale length NGC3627 (face-on)

- Removed the bulge to get the diffuse emission.
- **$F = f_0 \exp(-r/r_0)$**

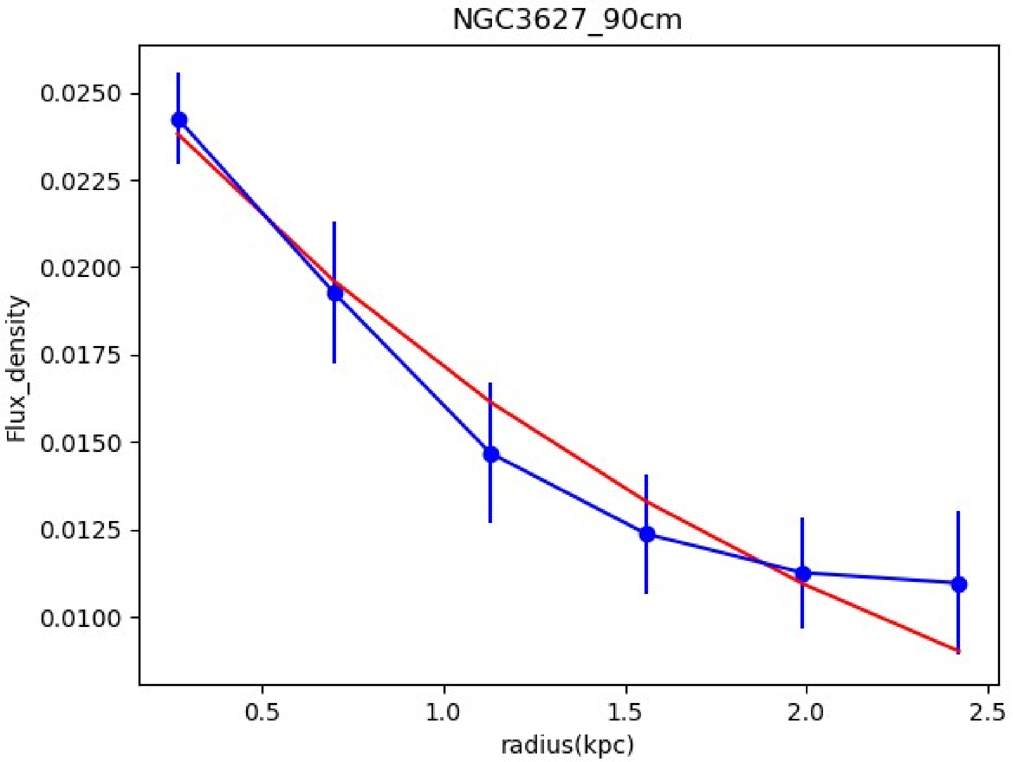

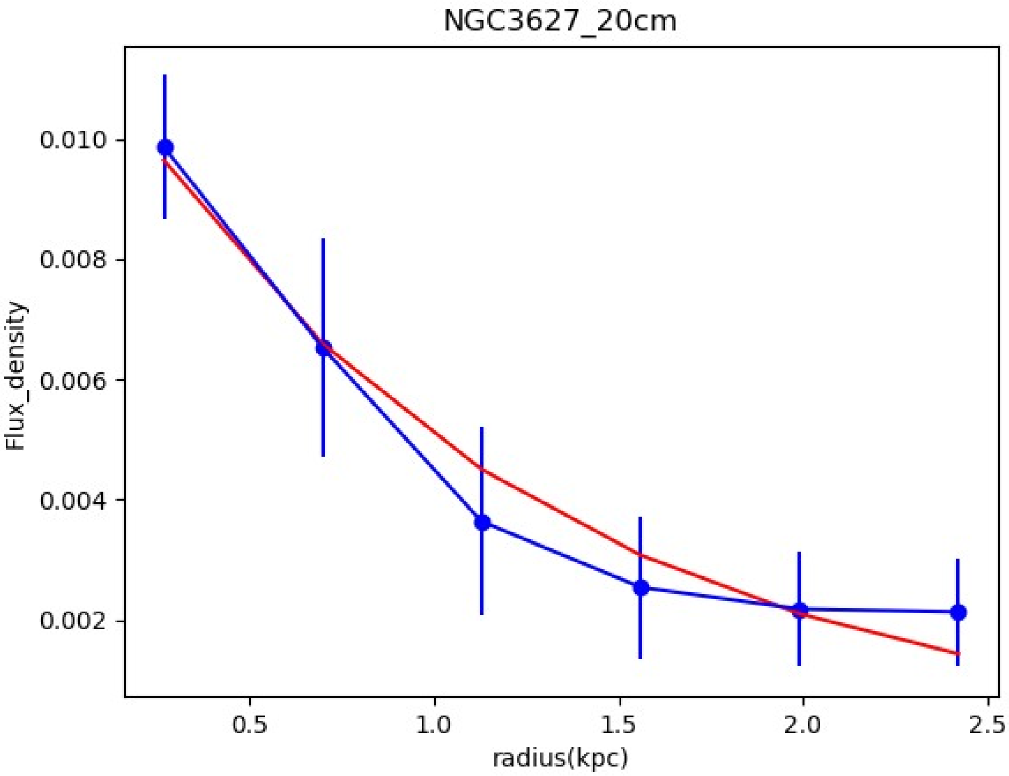

Thin disk approximation : Radial scale length NGC4826

- No separate bulge observed for NGC4826.
- **F =f_0 exp (-r/r_0)**

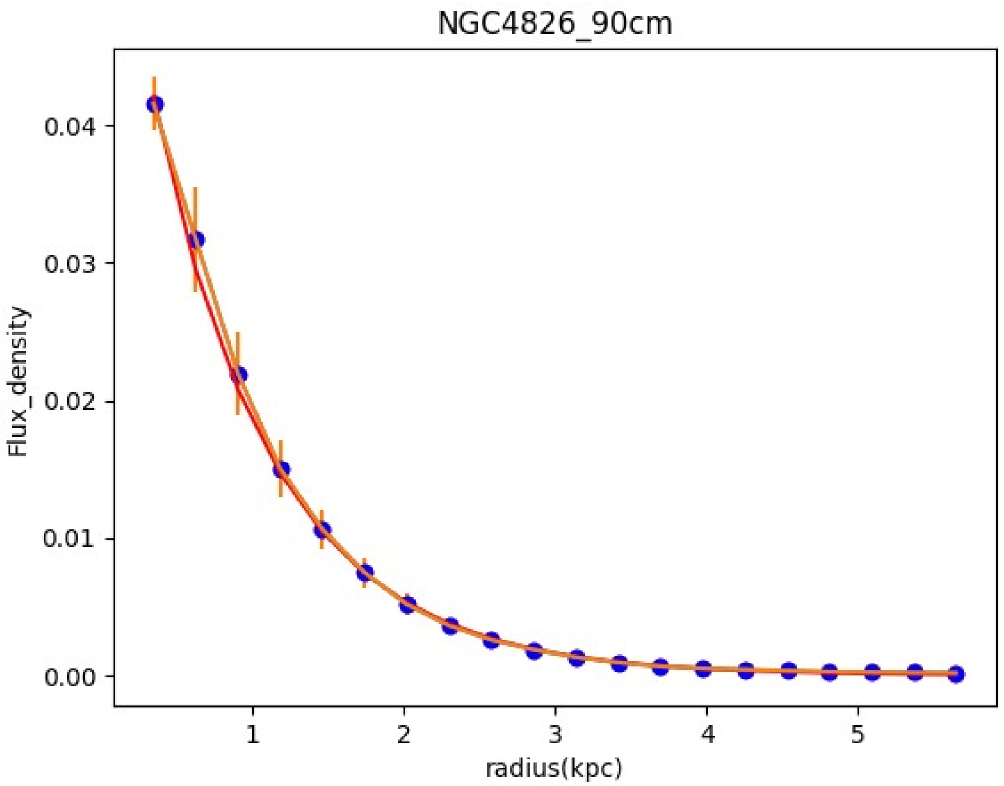

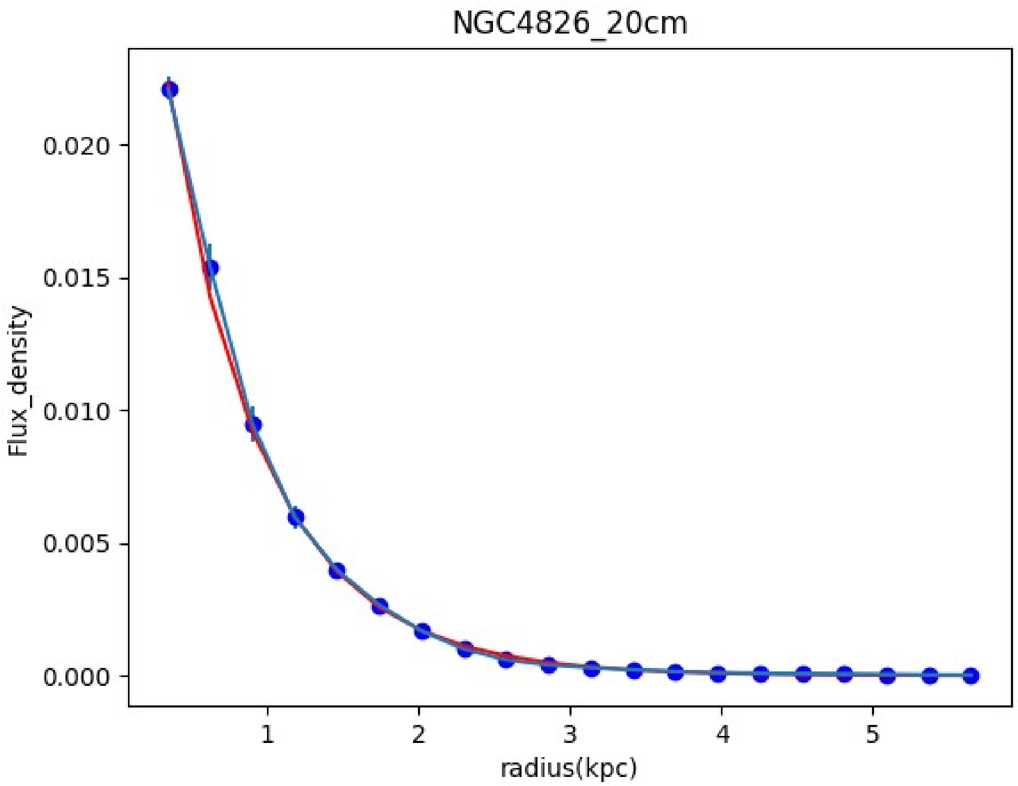

Thin disk approximation : Radial scale length

- **Face-on galaxies :**

Galaxy	Scale length 90cm(kpc)	Scale length error(kpc)	Scale length 20cm(kpc)	Scale length error(kpc)	$l_{diff, 90} / l_{diff, 20}$
NGC5194	5.2	0.02	1.95	0.015	2.66
NGC3627	2.21	0.2	1.12	0.11	1.97
NGC4826	3.02	0.17	1.88	0.09	1.60

- **Diffusion model:** $l_{\mathrm{diff}} \sim (D\ \tau)^{0.5}$ → $l_{diff, 90} / l_{diff, 20} = 1.4$

- **Alfven wave:** $l_{\mathrm{A}} = v_{\mathrm{A}} t_{\mathrm{syn}}.$ → $l_{A, 90} / l_{A, 20} = 2.0$

- **For three galaxies, scale length ratio is larger than that expected from simple diffusion estimation.**

Thick disk approximation: nearly edge-on galaxies

- **Simulate galaxy model:**
  - Simulate galaxy distribution on a 3D meshgrid with distribution function:

    $$\mathbf{I = I_0 \exp(-(r/r_0)^2) \exp(-z/h)}$$

  - Rotate this model galaxy by the inclination angle θ.
  - Convolve gaussian beam with the model galaxy.

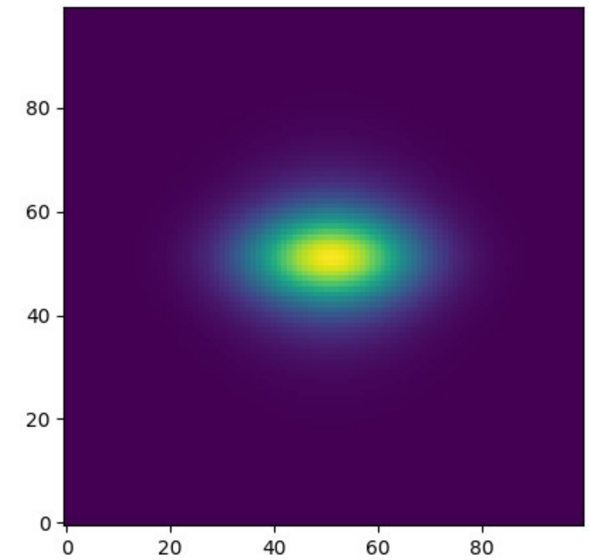

- **Observed radio map:**
- Rotate the map by the position angle of the galaxy to a horizontally orientated major axis.
- **Subtract** the model map from the observed radio map.
- **Markov chain Monte Carlo** (**MCMC**) methods to estimate free parameters : $\mathbf{I_0}$, $\mathbf{r_0}$, **h** and **θ** .   (**Foreman-Mackey et al. 2013**)

MCMC : results

- **Nearly edge-on galaxies :**

Galaxy	Scale length (kpc)	Scale length error (kpc)	Scale height (kpc)	Scale height error (kpc)
NGC2683	3.82	+0.13 -0.16	1.27	+ 0.05 -0.05
NGC4096	4.40	+0.30 -0.50	1.50	+0.15 -0.12
NGC4490	4.81	+0.45 -0.38	1.58	+0.13 -0.16

- CHANG-ES **:** Sample average scale heights in C and L bands are 1.1 ± 0.3 kpc and 1.4 ± 0.7 kpc.

Conclusion and future work

- The strengths of the total magnetic field decreases by ~40–50 per cent from center to edge of the galaxies.
- For three face on galaxies , radial scale length ratio is larger than that expected from simple diffusion estimates.
- Vertical scale height increases with decreasing frequency. Scale height at 20 cm will be determined to study the propagation of particles in more detail.
- uGMRT observation of another 17 galaxies between 300-500 MHz of different hubble types in last cycle of GMRT.
- Analyse CO data to study neutral gas properties of those galaxies.
- SFR estimation combining Ha + IR and FUV + IR to exploit the complementary strengths at different wavebands (kennicutt 2012). Study magnetic field – SFR correlations.

Energy density in magnetic field and gas

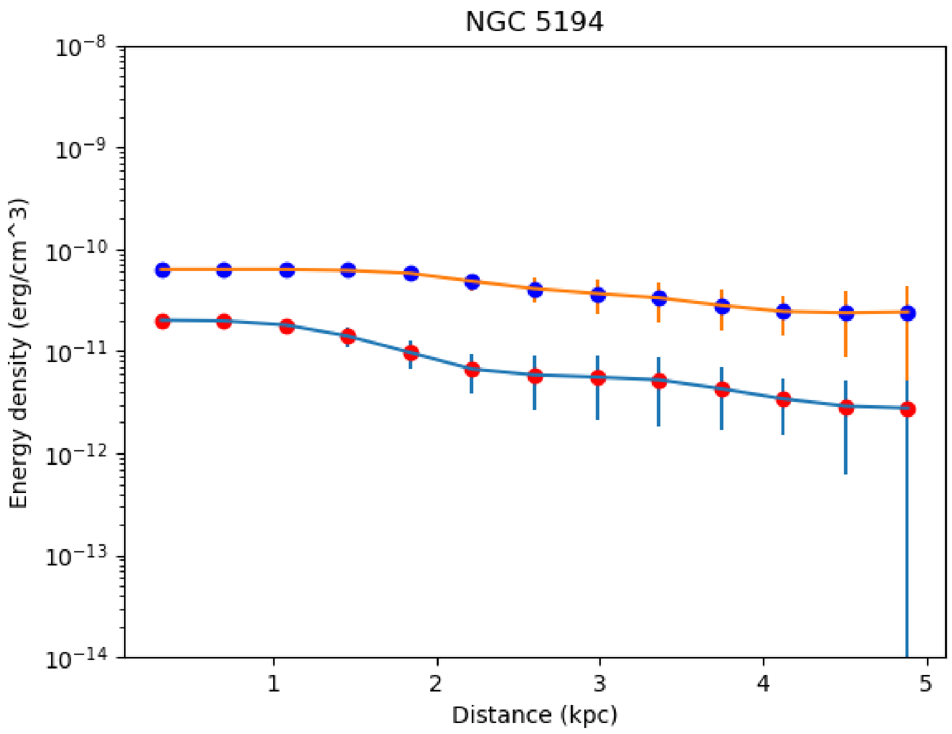

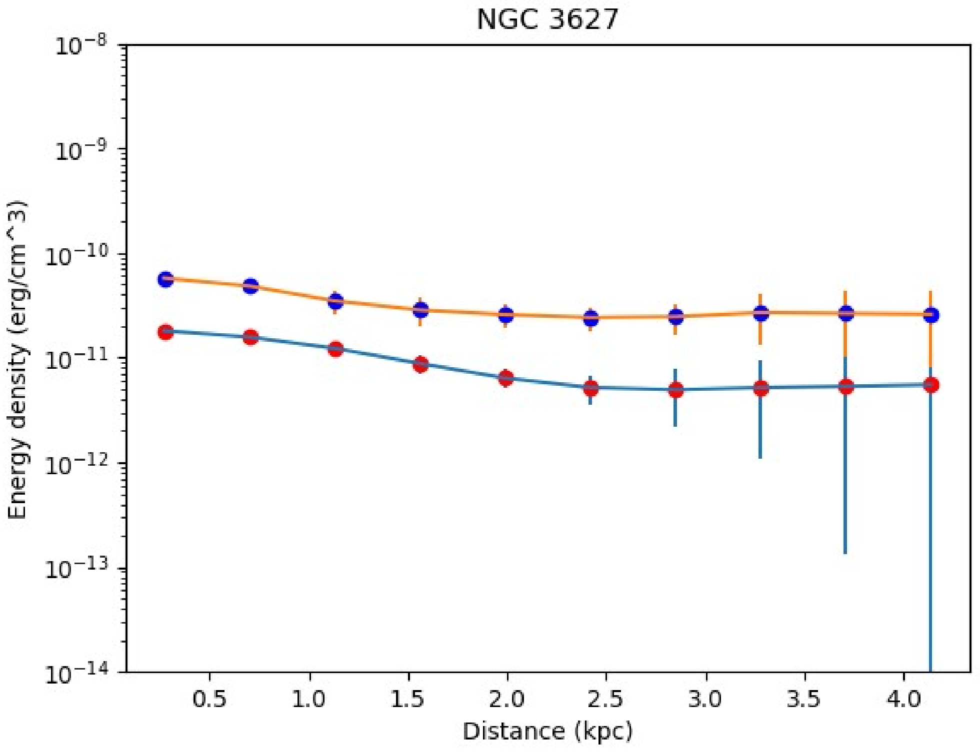

Corner plot

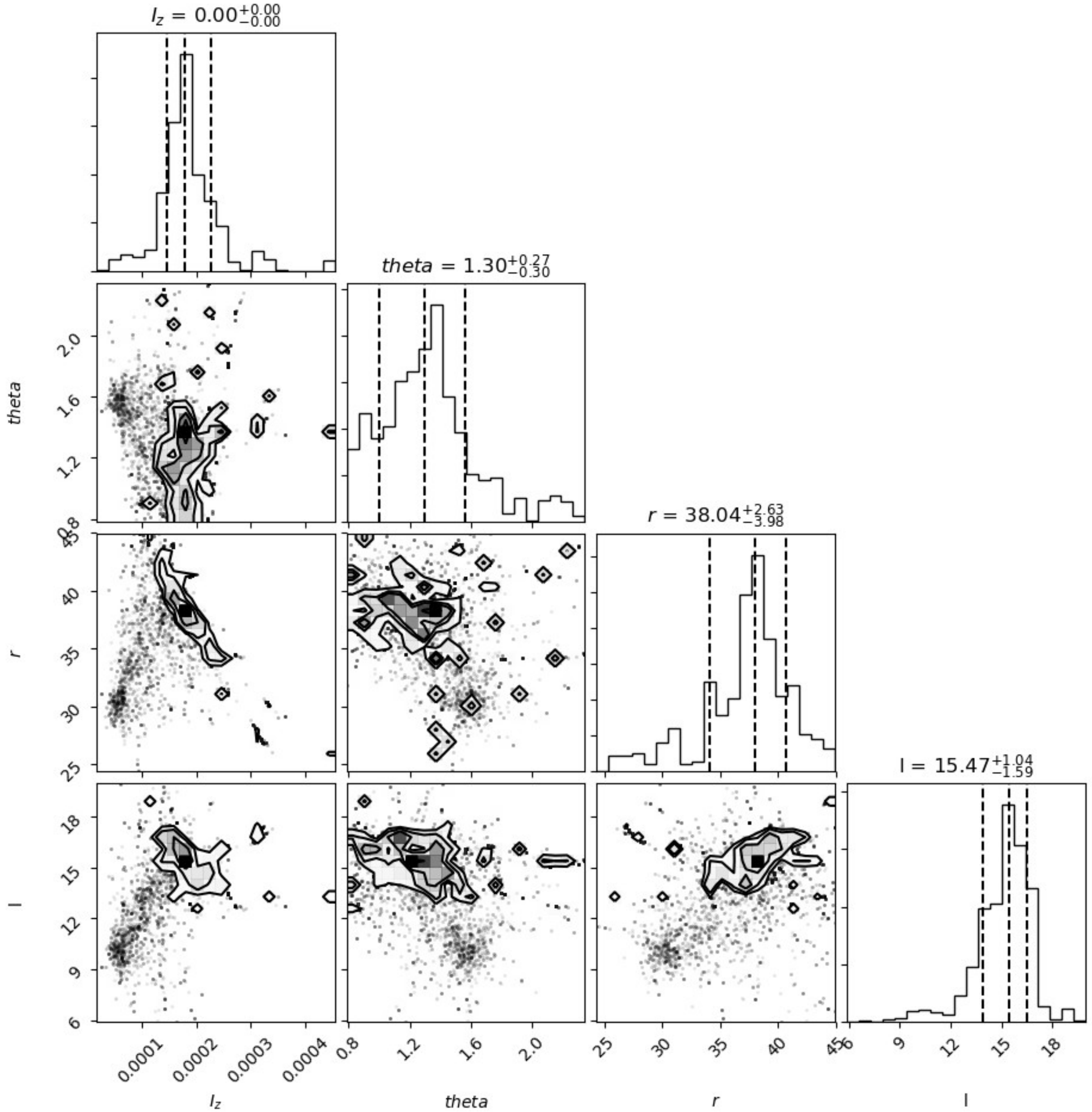

$I_z = 0.00^{+0.00}_{-0.00}$
$theta = 1.30^{+0.27}_{-0.30}$
$r = 38.04^{+2.63}_{-3.98}$
$l = 15.47^{+1.04}_{-1.59}$
theta
r
l
I_z
theta
r
l